

Ferroelectric and ferromagnetic properties in BaTiO₃ thin films on Si (100)

Srinivasa Rao Singamaneni, Sandhyarani Punugupati, John T. Prater, Frank Hunte, and Jagdish Narayan

Citation: *Journal of Applied Physics* **116**, 094103 (2014); doi: 10.1063/1.4894508

View online: <http://dx.doi.org/10.1063/1.4894508>

View Table of Contents: <http://scitation.aip.org/content/aip/journal/jap/116/9?ver=pdfcov>

Published by the [AIP Publishing](#)

Articles you may be interested in

Ferroelectric and ferromagnetic properties of epitaxial BiFeO₃-BiMnO₃ films on ion-beam-assisted deposited TiN buffered flexible Hastelloy

J. Appl. Phys. **115**, 17D913 (2014); 10.1063/1.4869438

Compositional engineering of BaTiO₃/(Ba,Sr)TiO₃ ferroelectric superlattices

J. Appl. Phys. **114**, 104102 (2013); 10.1063/1.4820576

Upward ferroelectric self-polarization induced by compressive epitaxial strain in (001) BaTiO₃ films

J. Appl. Phys. **113**, 204105 (2013); 10.1063/1.4807794

Coherent in-plane tensile strain in perovskite Ba_{0.8}Sr_{0.2}TiO₃ films on spinel MgAl₂O₄ substrates

Appl. Phys. Lett. **100**, 032902 (2012); 10.1063/1.3677938

Microstructure and ferroelectric properties of low-fatigue epitaxial, all (001)-oriented (Bi, La)₄Ti₃O₁₂Pb (Zr_{0.4}Ti_{0.6})O₃ (Bi, La)₄Ti₃O₁₂ trilayered thin films on (001) SrTiO₃ substrates

J. Appl. Phys. **98**, 014101 (2005); 10.1063/1.1946913



AIP | Journal of Applied Physics



Journal of Applied Physics is pleased to announce **André Anders** as its new Editor-in-Chief

Ferroelectric and ferromagnetic properties in BaTiO₃ thin films on Si (100)

Srinivasa Rao Singamaneni,^{1,2,a)} Sandhyarani Punugupati,² John T. Prater,^{1,2} Frank Hunte,² and Jagdish Narayan²

¹Materials Science Division, Army Research Office, Research Triangle Park, North Carolina 27709, USA

²Department of Materials Science & Engineering, North Carolina State University, Raleigh, North Carolina 27695, USA

(Received 12 June 2014; accepted 21 August 2014; published online 4 September 2014)

In this paper, we report on the epitaxial integration of room temperature lead-free ferroelectric BaTiO₃ thin (~1050 nm) films on Si (100) substrates by pulsed laser deposition technique through a domain matching epitaxy paradigm. We employed MgO and TiN as buffer layers to create BaTiO₃/SrRuO₃/MgO/TiN/Si (100) heterostructures. C-axis oriented and cube-on-cube epitaxial BaTiO₃ is formed on Si (100) as evidenced by the in-plane and out-of-plane x-ray diffraction, and transmission electron microscopy. X-ray photoemission spectroscopic measurements show that Ti is in 4(+) state. Polarization hysteresis measurements together with Raman spectroscopy and temperature-dependent x-ray diffraction confirm the room temperature ferroelectric nature of BaTiO₃. Furthermore, laser irradiation of BaTiO₃ thin film is found to induce ferromagnetic-like behavior but affects adversely the ferroelectric characteristics. Laser irradiation induced ferromagnetic properties seem to originate from the creation of oxygen vacancies, whereas the pristine BaTiO₃ shows diamagnetic behavior, as expected. This work has opened up the route for the integration of room temperature lead-free ferroelectric functional oxides on a silicon platform. © 2014 AIP Publishing LLC.

[<http://dx.doi.org/10.1063/1.4894508>]

I. INTRODUCTION

Ferroelectric perovskites have many unique physical properties that make them candidate materials for various applications such as microphotonics,¹ nonvolatile memories,² and dynamic random access memories (DRAMs).³ BaTiO₃ (BTO) is the prototypical ferroelectric perovskite, most studied perovskite-type ferroelectrics because of its important electrical and optical properties. In BTO, the TiO₆ octahedra are linked in a regular cubic array forming the high-symmetry *Pm3m* prototype in the paraelectric state. In the ferroelectric state below the Curie temperature $T_C \sim 110^\circ\text{C}$, a spontaneous polarization arises due to the noncentrosymmetric displacement of Ti⁴⁺ and O²⁻ ions relative to Ba²⁺ ions (*P4mm*).

To date, most of the BTO epitaxial thin films have been deposited on SrTiO₃ (STO)⁴⁻⁶ and MgO^{7,8} and DyScO₃ (Ref. 9) substrates, which are insulators and expensive with limited substrate size, and, more importantly, incompatible with the present day CMOS devices. To address this, a few studies^{10,11} have reported on the deposition of BTO thin films on buffered (with SrTiO₃) Si (100) by taking advantage of the molecular beam epitaxy (MBE) technique, that avoids the formation of an interfacial SiO_x layer. For instance, recently, a group¹⁰ from IBM reported on the deposition of BTO thin film on Si (100), in which, they have used MBE to deposit a STO buffer layer on Si (100). As early¹² as 1995, the epitaxial growth of BTO on Si (100) has been reported, deposited by pulsed laser deposition (PLD) using TiN as a buffer layer, in which, TiN was used as both top and bottom electrodes. Unfortunately, that study did not confirm the ferroelectric nature of BTO,

probably due to the non-ideal electrodes. In their work, the BTO microstructure was not well characterized. In another report,¹³ vertically aligned thin film nanostructures of BTO-CeO₂ have been deposited on a silicon substrate.

To better address the above issues, in this letter, we have demonstrated the ferroelectric properties of lead-free epitaxial BaTiO₃ thin films deposited by PLD assisted by domain matching epitaxy (DME), integrated with the silicon platform using high temperature x-ray diffraction (XRD), cross sectional transmission electron microscope (TEM), Raman spectroscopy, and polarization hysteresis measurements. BaTiO₃/SrRuO₃ (SRO)/MgO/TiN/Si (100) heterostructures have been characterized to establish structure property correlations. Also, we have shown that laser annealing/irradiation of BTO thin film introduces ferromagnetic-like features, but, it affects adversely the ferroelectric behavior whereas the pristine BTO films preserved their diamagnetic characteristics. The DME is very promising approach for integrating systems of varying misfits, which in previous work we have successfully used to integrate other room temperature ferroelectric materials such as BiFeO₃ (Ref. 14) and PZT.¹⁵

In this paper, we have prepared BaTiO₃/SrRuO₃/MgO/TiN/Si (100) epitaxial thin film heterostructures by PLD, in which SrRuO₃ acts as an electrode with MgO and TiN as buffer layers. Since silicon has a higher refractive index than BTO, a low refractive index cladding layer is needed between the silicon and the BTO for wave guiding, particularly for microphotonic applications. The cladding layer also needs to be epitaxial in order to achieve epitaxy of the BTO layer. Moreover, it should be electrically insulating. MgO meets all these requirements and was chosen for the buffer layer in the current work. To describe the deposition procedure briefly, TiN, MgO, and BTO targets were ablated sequentially in the

^{a)}ssingam@ncsu.edu

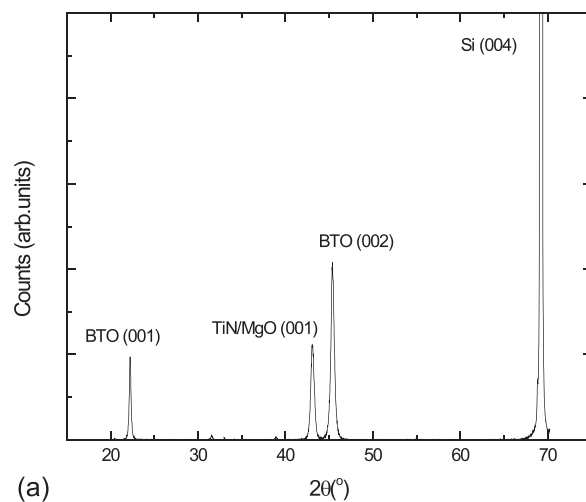
same chamber using a rotating target assembly. The deposition of the TiN layer was performed at 625 °C in vacuum (1×10^{-6} Torr). Following TiN deposition, the first few mono layers (for about 500 pulses) of MgO were deposited under vacuum (1×10^{-6} Torr) at 575 °C. The remaining MgO was then deposited at the same temperature under an oxygen pressure of 6×10^{-4} Torr. Finally, BTO deposition was carried out under O₂ partial pressure of 2×10^{-1} Torr at a substrate temperature of 700 °C. The energy density and pulse frequency were 1.5–2.5 J/cm² and 10 Hz, respectively. Once completed, the samples were cooled slowly to ambient temperature under the same O₂ partial pressure. For ferroelectric measurements, capacitor structures were made using SRO and Pt as bottom and top electrodes, respectively. A very important issue is the available carrier density within the electrodes in contact with the ferroelectric layer. We have chosen epitaxial SRO, which is known⁹ to provide up to 2×10^{22} carriers/cm³ on the bottom side and metallic Pt as the top electrode. This arrangement provides an ideal capacitor sandwich for perovskite ferroelectrics, because these electrodes are able to provide zero depolarization field within the BTO, which is important for measuring intrinsic ferroelectric hysteresis loops. For cross-section TEM sample preparation, we have followed the conventional mechanical polishing and ion milling process.

II. EXPERIMENTAL

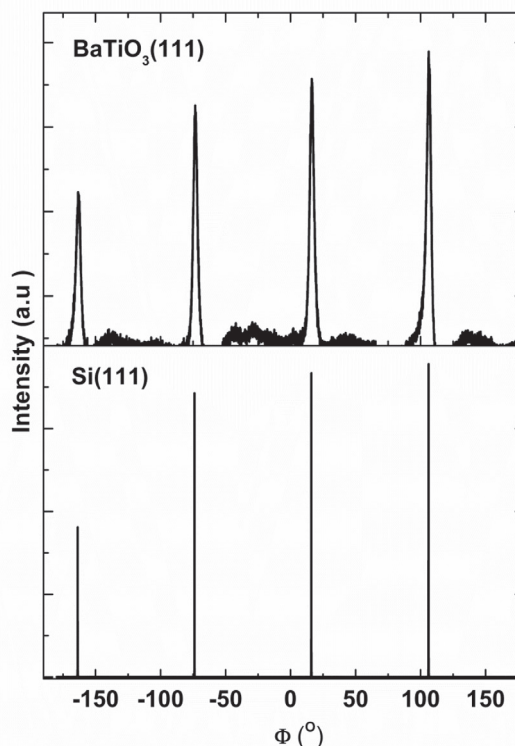
The structures of BTO samples were characterized by XRD θ - 2θ scans using a Rigaku x-ray diffractometer with Cu K α radiation ($\lambda = 1.5418$ Å). X-ray photoemission spectroscopy (XPS) was employed on a SPECS FlexMod system equipped with an Al K α monochromatic x-ray source (1486.7 eV) to identify (if at all) the surface metal contaminations and to probe the oxidation states of various elements in the BTO. XRD measurements to obtain above-room temperature (RT = 25 °C), the sample was heated in a high temperature capable dispex with a maximum of 700 °C, and a temperature control of ± 0.5 °C. The microstructures of these films were characterized using a JEOL-2000FX TEM. A detailed atomic-resolution study at BaTiO₃/MgO interface was performed, using a JEOL-2010F high resolution TEM (HRTEM), equipped with a Gatan image filter tuning attachment, which has a point-to-point resolution of 0.18 nm. Raman spectra were recorded using a Horiba Jobin Yvon T64000 triple spectrometer equipped with a multichannel charge-coupled device detector. Spectra were recorded in backscattering geometry at 300 K. For excitation, the 633 nm He–Cd laser line was used with a power density of 0.4 W/mm², low enough to avoid any noticeable local heating. For ferroelectric measurements, we have used Radiant technologies premier II ferroelectric tester.

III. RESULTS AND DISCUSSION

Figure 1(a) presents a θ - 2θ XRD pattern of the BTO/MgO/TiN/Si (100) heterostructure. No evidence of additional phases or interfacial reaction products was observed in the XRD pattern. It is evident from this pattern that all the layers show preferential (00 l) orientation, suggesting either the textured or epitaxial growth of the multilayered structure. From



(a)



(b)

FIG. 1. (a) Typical θ - 2θ (out of plane) XRD pattern of BTO sample showing high quality, single phase and (00 l) films of BTO (b) ϕ -scan patterns of BTO and Si of (111) reflection collected from sample A at $2\theta = 39.46^\circ$, $\omega = 19.73^\circ$ and $\chi = 55.00^\circ$ for BFO and $2\theta = 28.46^\circ$, $\omega = 14.23^\circ$ and $\chi = 54.74^\circ$ for Si (100). This pattern shows 4 peaks separated by $\sim 90^\circ$ indicating its pseudo cubic/rhombohedral symmetry, establishing the cube-on-cube relationship with the underlying substrate Si (100). The ϕ -scan XRD pattern of MgO/TiN layers is shown in the supplemental information¹⁶ (Fig. S1), inferring that all these four layers are epitaxial. The rocking curve with FWHM of $1-1.3^\circ$ of BTO (002) diffraction peak is shown in supplemental information¹⁶ (see Fig. S2).

the 2θ XRD data for the (002) peak, we determined the out-of-plane (OOP) lattice parameter of BTO to be 3.996 Å. The epitaxial growth and the in-plane (IP) orientation of all the three layers were studied in detail by means of ϕ -scan XRD. As depicted in Fig. 1(b), the ϕ -scan patterns of (111) reflection for BTO and Si were collected. This pattern shows 4

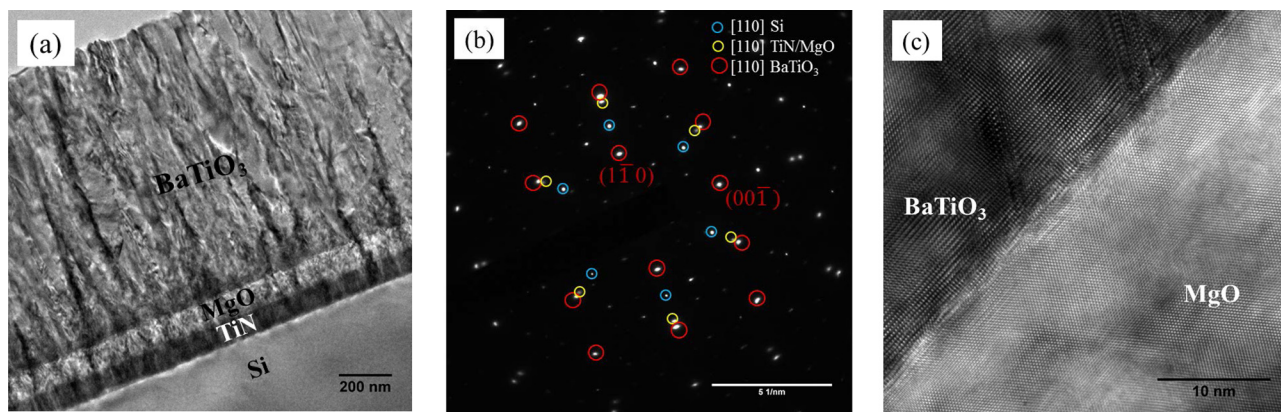


FIG. 2. (a) Bright field cross-section TEM image taken from BTO sample, where BTO (~ 1050 nm) film was grown at 700°C . All 3-layers are marked. The scale bar is 200 nm (b) (110) zone-axis pattern (ZAP) for BTO/MgO interface (c) HRTEM image of BTO (1050 nm)/MgO (95 nm) interface.

peaks separated by $\sim 90^\circ$ indicating its cubic symmetry and establishing the cube-on-cube relationship of the BTO with the underlying substrate Si (100). The φ -scan XRD patterns of MgO/TiN layers are shown in the supplemental information¹⁶ (see Fig. S1) confirming that all 3 layers are grown epitaxially cube-on-cube, i.e., (001)Epilayer// (001)Buffer and $[110]$ Epilayer// $[110]$ Buffer. Figure S2 shows¹⁶ the rocking curve (to evaluate mosaicity, which is, angular dispersion along the growth direction) of the BTO (002) peak; where the full width at half maximum (FWHM) is about 1.4° . This mosaic spread can be attributed to the large lattice mismatch between MgO and BTO (15.3% with a axis and 24.2% with c axis) which must promote the rotations between islands.

Fig. 2(a) is a typical bright-field cross-section TEM image of the sample, in which the BTO/MgO/TiN/Si (100) layers are labeled. The thicknesses of BTO, MgO, and TiN are determined as ~ 1050 , 95, and 85 nm, respectively. The $\langle 110 \rangle$ zone axis electron diffraction pattern of the BTO/MgO/TiN/Si region is shown in Fig. 2(b). Due to the close lattice match between MgO and TiN, the low order diffraction spots in Fig. 2(b) were indistinguishable. The alignment of two sets of diffraction spots proves the cube-on-cube epitaxial relationship between the top two layers. It should be emphasized that the epitaxial growth of BTO/MgO on Si (100) is possible due to the epitaxial growth of large mismatched system based on the DME paradigm, e.g., TiN grows on Si (100) such that four lattice constants of TiN match with three of Si (100). An important feature of DME concept is that most of the strain is relieved almost immediately upon initiation of growth, i.e., within the first couple of monolayers of growth. In this way, lattice misfit strain accommodation is confined to the interface making it possible for the rest of the film to be grown free of defects and lattice strain. More details on TiN/Si deposition can be found in our earlier work.¹⁷ Fig. 2(c) presents typical high resolution electron microscopic (HREM) images taken at the BTO/MgO interface, showing the presence of misfit dislocations at the interface, and are found to be absent as the film grows thicker.

To identify the ferroelectric phase transition, the temperature dependence of the out-of-plane lattice parameters of the films was measured with a variable-temperature four-circle x-ray diffractometer equipped with a two dimensional

(2D) area detector with an angular resolution of 0.02° . The out of plane lattice parameters of BTO films as a function of temperature obtained from the XRD measurements are given in Fig. 3. As it can be seen, BTO undergoes a ferroelectric transition at about 130°C , in agreement with the literature data.⁷ The XRD patterns as a function of temperature are shown in the supplementary information¹⁶ (see Fig. S3). Similar results were obtained when the measurements were done during the cooling down cycle (data not shown).

The Raman spectrum of the epitaxial BTO thin films recorded at room temperature is presented in Fig. 4. The MgO/TiN buffer layers have no Raman lines in the spectral range studied and therefore it does not interfere with the BTO film. Laser power density (0.7 W/cm^2) at the sample surface was adjusted to be low enough to avoid local heating. As it can be seen, the spectral features are consistent with the previous studies on BTO film. For identification of the observed phonon peaks, we compared the measured spectra with Raman spectra of bulk single crystal¹⁸ and epitaxial thin film¹⁹ BTO from the literature reports. The first-order Raman peaks of BTO are seen, indicating that the film is polar at room temperature. The most distinct BTO phonon lines were

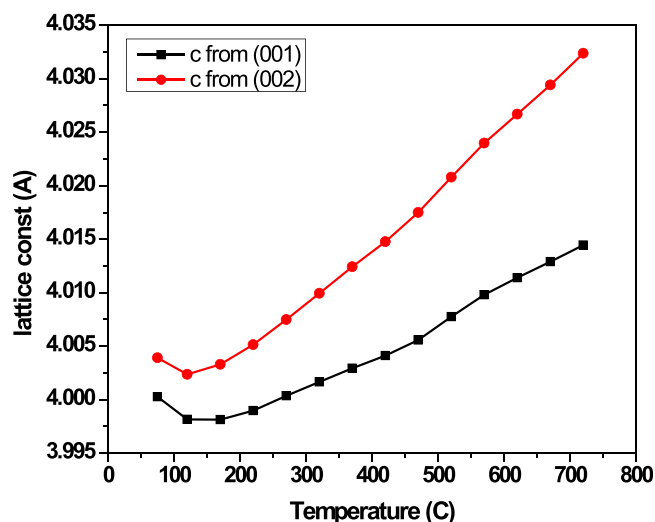


FIG. 3. Temperature dependence of the out of plane lattice parameter of the BTO thin film collected for (001) and (002) reflections.

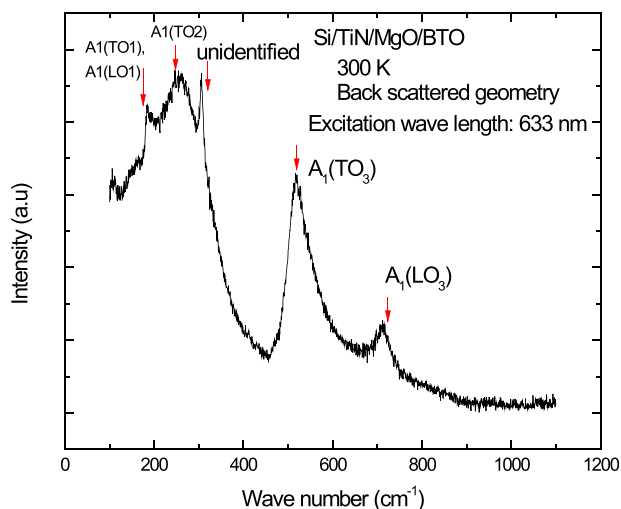


FIG. 4. Room temperature Raman spectra of the BTO thin film.

observed at about 180, 475, and 520 cm^{-1} , and attributed to TO1 + LO1, LO2, and TO3 modes of A1 symmetry, respectively. The A1(LO) modes are Raman active. The presence of the A1(TO) modes is likely due to deviations from true back-scattering. Slightly lower TO3 phonon frequency in this BTO thin film (520 cm^{-1}) compared to bulk BTO (522 cm^{-1}) is likely due to the tensile strain. A peak at 300 cm^{-1} seen in the spectra of the BTO film corresponds to the A1(TO2) mode of the tetragonal BTO.

Polarization hysteresis measurements were made on 250- μm -diameter capacitors of relaxed BTO thin films sandwiched between Pt top and bottom electrodes of the conducting perovskite oxide SrRuO₃. Figure 5 shows the representative ferroelectric hysteresis loops measured on the BTO devices. These measurements have been reproduced on several devices fabricated on two identical Si (100) substrates as a function of frequency ranging from 2 to 20 kHz, voltage ranging from -10 to +10 V. As it can be noticed, the polarization reversal exhibits a clear memory and near-saturation. The coercive voltage (V_c) is ~ 0.9 V (measured on the negative voltage axis). Most importantly, the coercive voltage is

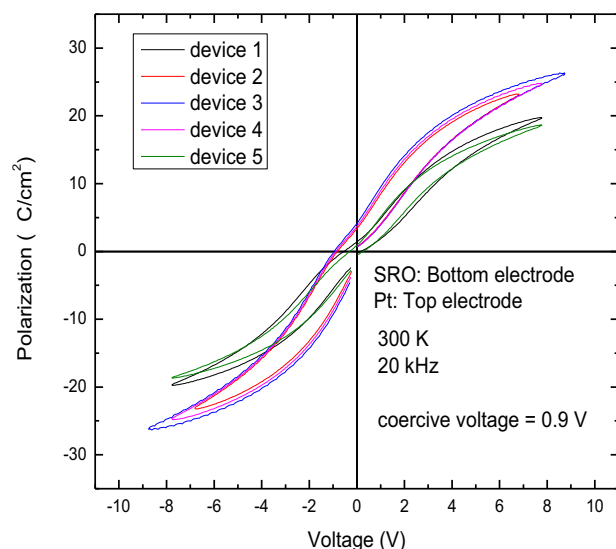


FIG. 5. P-V hysteresis measurements collected for several BTO devices.

significantly lower than the ones (5–10 V) reported on 40 nm-thick BTO thin films deposited on Si (100) by other groups.¹⁰ Also, the observed remanent polarization (4–5 $\mu\text{C}/\mu\text{m}^2$) is in good agreement with the values (1–8 $\mu\text{C}/\mu\text{m}^2$) previously reported^{20,21} for the BTO thin films, but, inferior (24 $\mu\text{C}/\mu\text{m}^2$) to those of BTO single crystal,²² most likely due to microscopic structural variations and the stoichiometry of the films.²³ As it can be noticed, the hysteresis loops are shifted in the negative voltage direction. This imprint effect is probably due to the asymmetric interfacial properties⁹ of the top and bottom electrodes to the BTO films. The pinching nature (near the origin) of ferroelectric loops could have originated from the existence of a distributed ion of switchable dipolar defects.²⁴ The ferroelectric loops were measured for about 50 cycles with no indication of polarization degradation (data not shown), i.e. the devices retained their pristine characteristics.

Isothermal (5 K) in-plane SQUID magnetometry measurements were performed on pristine and laser annealed BTO films. As shown in Fig. 6, we found that the laser annealed (with 20 pulses) films show ferromagnetic-like features, with clear saturation and a coercive field of 200 Oe, in contrast to the pristine BTO film which displays diamagnetic behavior (see the inset of Fig. 6). In addition, we have tested (data not shown) BTO films irradiated with 10 number of laser pulses and found that they did not show such ferromagnetic features. Concurrently, both laser annealed BTO films failed to show good ferroelectric characteristics¹⁶ (see, supplementary information Fig. S4) due to high leakage current, probably, due to the introduction of oxygen vacancies upon laser annealing. Survey scans of XPS spectra¹⁶ (see Fig. S5) collected on pristine and laser annealed BTO films did not show indications of surface contaminations. High resolution XPS spectra¹⁶ (see supplementary information Fig. S6) indicate that Ti is in +4, and, did not detect any element other than Ba, Ti, O, and environmental carbon. However,

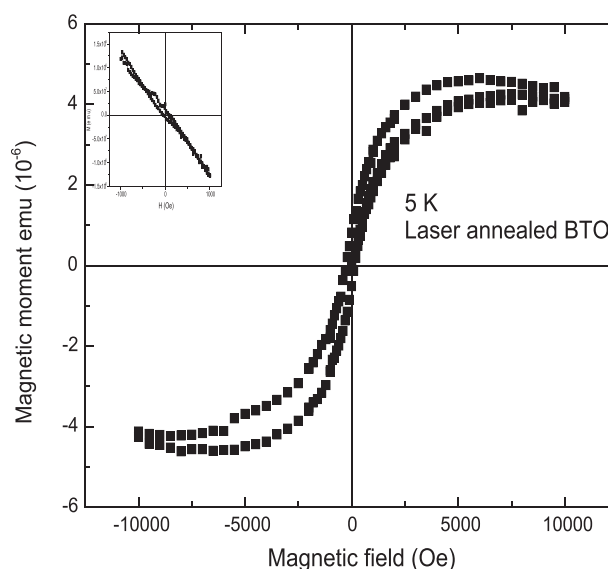


FIG. 6. In-plane isothermal (5 K) M-H measurements collected for laser annealed (20 pulses) BTO thin films showing ferromagnetic-like behavior. The inset shows the diamagnetic behavior pristine BTO. The magnetic field is applied along $\langle 100 \rangle$ direction of the sample. 10-pulse laser irradiated BTO shows no ferromagnetic behavior (not shown).

we see a clear shift (marked in red) of the oxygen peak upon laser annealing. XRD patterns of BTO (002) reflection before and after laser annealing are compared¹⁶ (see supplementary information Fig. S7). We have noticed a peak broadening from 0.40° to 0.54° without peak shift. MgO and TiN were tested to be non-magnetic. The fact that the XRD and XPS data did not reveal any indication of secondary impurities before or after laser annealing, and we see no ferroelectric features after laser irradiation, we believe that oxygen vacancies are the sources of the leakage currents (adversely affecting ferroelectricity) and also are responsible for the observed ferromagnetic features, similar to many other reports.^{25,26}

IV. SUMMARY

In summary, we have integrated room temperature ferroelectric epitaxial BaTiO₃ using pulsed laser deposition technique assisted by domain matching epitaxy paradigm onto a silicon platform. The details of epitaxial growth in BTO/SRO/MgO/TiN/Si (100) heterostructures have been studied using x-ray diffraction and cross-sectional imaging and diffraction. We have demonstrated its ferroelectric nature using high temperature x-ray diffraction, Raman spectroscopy, and polarization hysteresis measurements. The coercive voltage is found as less than 1 V. In addition, we have shown that the laser annealed BaTiO₃ shows ferromagnetic-like behavior whereas the pristine BaTiO₃ is diamagnetic. But, laser annealing adversely affects the ferroelectric behaviour. This work forms a significant step toward the epitaxial integration of lead-free room temperature ferroelectric oxides on silicon platform for memory applications and cautions that the laser treatment destroys the ferroelectric characteristics.

ACKNOWLEDGMENTS

S.S.R. acknowledges National Academy of Science (NAS), USA, for awarding the NRC postdoctoral research associate fellowship. The authors are pleased to acknowledge the support of the Army Research Office under Grant W911NF-04-D-0003. We thank C. T. Shelton and J.-P. Maria for valuable help while depositing the top electrodes. We thank Dr. Jacob Jones and Jason Nikkel for their help in high temperature XRD measurements. Also, the authors acknowledge the use of the Analytical Instrumentation Facility (AIF) at North Carolina State University, which is supported by the State of North Carolina and the National Science Foundation.

¹F. Niu, A. R. Teren, B. H. Hoerman, and B. W. Wessels, *Mat. Res. Soc. Symp. Proc.* **637**, E1.9 (2001).

- ²R. Guo, L. You, Y. Zhou, Z. S. Lim, X. Zou, L. Chen, R. Ramesh, and J. Wang, *Nat. Commun.* **4**, 1990 (2013).
- ³M. Bibes and A. Barthélémy, *Nature Mater.* **7**, 425 (2008).
- ⁴D. A. Tenne, P. Turner, J. D. Schmidt, M. Biegalski, Y. L. Li, L. Q. Chen, A. Soukiassian, S. Trolier-McKinstry, D. G. Schlom, X. X. Xi, D. D. Fong, P. H. Fuoss, J. A. Eastman, G. B. Stephenson, C. Thompson, and S. K. Streiffer, *Phys. Rev. Lett.* **103**, 177601 (2009).
- ⁵C. Li, Z. Chen, D. Cui, Y. Zhou, H. Lu, C. Dong, F. Wu, and H. Chen, *J. Appl. Phys.* **86**, 4555 (1999).
- ⁶T. Shimizu, D. Suwama, H. Taniguchi, T. Taniyama, and M. Itoh, *J. Phys.: Condens. Matter* **25**, 132001 (2013).
- ⁷M. El Marssi, F. Le Marrec, I. A. Lukyanchuk, and M. G. Karkut, *J. Appl. Phys.* **94**, 3307 (2003).
- ⁸D. L. Kaiser, M. D. Vaudin, L. D. Rotter, Z. L. Wang, J. P. Cline, C. S. Hwang, R. B. Marinenko, and J. G. Gillen, *Appl. Phys. Lett.* **66**, 2801 (1995).
- ⁹K. J. Choi, M. Biegalski, Y. L. Li, A. Sharan, J. Schubert, R. Uecker, P. Reiche, Y. B. Chen, X. Q. Pan, V. Gopalan, L.-Q. Chen, D. G. Schlom, and C. B. Eom, *Science* **306**, 1005 (2004).
- ¹⁰C. Dubourdieu, J. Bruley, T. M. Arruda, A. Posadas, J. Jordan-Sweet, M. M. Frank, E. Cartier, D. J. Frank, S. V. Kalinin, A. A. Demkov, and V. Narayanan, *Nat. Nanotechnol.* **8**, 748 (2013).
- ¹¹V. Vaithyanathan, J. Lettieri, W. Tian, A. Sharan, A. Vasudevarao, Y. L. Li, A. Kochhar, H. Ma, J. Levy, P. Zschack, J. C. Woicik, L. Q. Chen, V. Gopalan, and D. G. Schlom, *J. Appl. Phys.* **100**, 024108 (2006).
- ¹²M.-B. Lee, M. Kawasaki, M. Yoshimoto, and H. Koinuma, *Appl. Phys. Lett.* **66**, 1331 (1995).
- ¹³F. Khatkhatay, A. Chen, J. H. Lee, W. Zhang, H. Abdel-Raziq, and H. Wang, *ACS Appl. Mater. Interfaces* **5**, 12541 (2013).
- ¹⁴S. S. Rao, J. T. Prater, Fan Wu, C. T. Shelton, J.-P. Maria, and J. Narayan, *Nano Lett.* **13**, 5814 (2013).
- ¹⁵A. K. Sharma, J. Narayan, C. Jin, A. Kvit, S. Chattopadhyay, and C. Lee, *Appl. Phys. Lett.* **76**, 1458 (2000).
- ¹⁶See supplementary material at <http://dx.doi.org/10.1063/1.4894508> for XRD ϕ -scan pattern of MgO of (111) reflection collected from MgO/TiN/Si(100); the rocking curve of BTO (002) diffraction; the temperature dependent XRD pattern of BTO (001) and BTO (002) reflections; representative P-V hysteresis loops measured from pristine BTO device and laser annealed BTO devices; XPS survey scan collected from pristine and laser annealed BTO; high resolution XPS scan collected from pristine and laser annealed BTO; high resolution XRD pattern of BTO (002) reflection collected from the pristine and laser annealed BTO thin film.
- ¹⁷J. Narayan, P. Tiwari, X. Chen, J. Singh, F. L. Chowdhury, and T. Zheleva, *Appl. Phys. Lett.* **61**, 1290 (1992).
- ¹⁸J. D. Freire and R. S. Katiyar, *Phys. Rev. B* **37**, 2074 (1988).
- ¹⁹D. A. Tenne, X. X. Xi, Y. L. Li, L. Q. Chen, A. Soukiassian, M. H. Zhu, A. R. James, J. Lettieri, D. G. Schlom, W. Tian, and X. Q. Pan, *Phys. Rev. B* **69**, 174101 (2004).
- ²⁰L. Huang, Z. Chen, J. D. Wilson, S. Banerjee, R. D. Robinson, I. P. Herman, R. Laibowitz, and S. O'Brien, *J. Appl. Phys.* **100**, 034316 (2006).
- ²¹R. Thomas, V. K. Varadan, S. Komarneni, and D. C. Dube, *J. Appl. Phys.* **90**, 1480 (2001).
- ²²B. Jaffe, W. R. Cook, and H. Jaffe, *Piezoelectric Ceramics* (Academic, New York, 1971), p. 78.
- ²³A. P. Chen, F. Khatkhatay, W. Zhang, C. Jacob, L. Jiao, and H. Wang, *J. Appl. Phys.* **114**, 124101 (2013).
- ²⁴G. Robert, D. Damjanovic, and N. Setter, *Appl. Phys. Lett.* **77**, 4413 (2000).
- ²⁵R. Molaei, R. Bayati, S. Nori, D. Kumar, J. T. Prater, and J. Narayan, *Appl. Phys. Lett.* **103**, 252109 (2013).
- ²⁶M. R. Bayati, S. Joshi, R. Molaei, R. J. Narayan, and J. Narayan, *J. Appl. Phys.* **113**, 063706 (2013).